Development of Tumor Targeting Bioprobes (^{111}In-Chimeric L6 Monoclonal Antibody Nanoparticles) for Alternating Magnetic Field Cancer Therapy

Sally J. DeNardo,[1] Gerald L. DeNardo,[1] Laird A. Miers,[1] Arutselvan Natarajan,[1] Alan R. Foreman,[2] Cordula Gruettner,[3] Grete N. Adamson,[1] and Robert Ivkov[2]

Abstract **Objectives:** ^{111}In-chimeric L6 (ChL6) monoclonal antibody (mAb) – linked iron oxide nanoparticle (bioprobes) pharmacokinetics, tumor uptake, and the therapeutic effect of inductively heating these bioprobes by externally applied alternating magnetic field (AMF) were studied in athymic mice bearing human breast cancer HBT 3477 xenografts. Tumor cell radioimmunotargeting of the bioprobes and therapeutic and toxic responses were determined.

Methods: Using 1-ethyl-3-(3-dimethylaminopropyl)-carbodiimide HCl, ^{111}In-7,10-tetraazacyclododecane-*N, N′,N″,N‴*-tetraacetic acid-ChL6 was conjugated to the carboxylated polyethylene glycol on dextran-coated iron oxide 20 nm particles, one to two mAbs per nanoparticle. After magnetic purification and sterile filtration, pharmacokinetics, histopathology, and AMF/bioprobe therapy were done using ^{111}In-ChL6 bioprobe doses (20 ng/2.2 mg ChL6/ bioprobe), i.v. with 50 μg ChL6 in athymic mice bearing HBT 3477; a 153 kHz AMF was given 72 hours postinjection for therapy with amplitudes of 1,300, 1,000, or 700 Oe. Weights, blood counts, and tumor size were monitored and compared with control mice receiving nothing, or AMF or bioprobes alone.

Results: ^{111}In-ChL6 bioprobe binding *in vitro* to HBT 3477 cells was 50% to 70% of that of ^{111}In-ChL6. At 48 hours, tumor, lung, kidney, and marrow uptakes of the ^{111}In-ChL6 bioprobes were not different from that observed in prior studies of ^{111}In-ChL6. Significant therapeutic responses from AMF/bioprobe therapy were shown with up to eight times longer mean time to quintuple tumor volume with therapy compared with no treatment ($P = 0.0013$). Toxicity was only seen in the 1,300 Oe AMF cohort, with 4 of 12 immediate deaths and skin erythema. Electron micrographs showed bioprobes on the surfaces of the HBT 3477 cells of excised tumors and tumor necrosis 24 hours after AMF/bioprobe therapy.

Conclusion: This study shows that mAb-conjugated nanoparticles (bioprobes), when given i.v., escape into the extravascular space and bind to cancer cell membrane antigen, so that bioprobes can be used in concert with externally applied AMF to deliver thermoablative cancer therapy.

Heating living tissues to temperatures between 42°C and 46°C leads to inactivation of normal cellular processes in a dose-dependent manner described for decades as the classic tissue hyperthermia response (1, 2). Tissues reaching temperatures above this level have extensive necrosis known as thermal ablation. Evidence has long suggested that thermal ablation can provide an alternative therapeutic modality for cancer that has failed standard therapies (3, 4). Approaches to heat induction include ultrasound, laser, IR radiation, microwave, radio frequency, and alternating magnetic fields (AMF). Catheters and probes, as well as external transducers, have been used in attempts to deliver thermal therapy more selectively. Treatments with radio frequency and microwave therapies have suffered from energy deposition in intervening tissue; this limitation seems to arise from nonspecific heating, as the energy source is also the heat source. AMF responsive nanoparticles attached to antitumor monoclonal antibodies (mAb) may enable specific cancer cell thermal ablation. When given systemically, such mAb linked nanoparticles (bioprobes) can target the extravascular cancer cells selectively, enabling external AMF to induce heating of cancer cell bound bioprobes.

The degree to which this approach can be applied to cancer therapy depends on bioprobes, which, after i.v. injection, reach the cancer cells in effective concentrations for thermal ablation when AMF is provided from an external source, and respond to otherwise tolerable levels of AMF by rapidly releasing intolerable heat to the microenvironment.

Reported herein, ^{111}In-mAb – conjugated iron oxide nanoparticles, ^{111}In-bioprobes (Fig. 1), were studied to assess whether their *in vivo* tumor uptake was sufficient to achieve a therapeutic response from AMF with tolerable toxicity. We

Authors' Affiliations: [1]University of California, Davis, Sacramento, California; [2]Triton BioSystems, Inc., Chelmsford, Massachusetts; and [3]Micromod Partikeltechnologie GmbH, Rostock, Germany

Grant support: Triton BioSystems, Inc.

Presented at the Tenth Conference on Cancer Therapy with Antibodies and Immunoconjugates, October 21-23, 2004, Princeton, New Jersey.

Requests for reprints: S.J. DeNardo, Radiodiagnosis and Therapy, 1508 Alhambra Boulevard 3100, Sacramento, CA 95816. Phone: 916-734-3787; Fax: 916-451-2857; E-mail: sjdenardo@ucdavis.edu.

doi:10.1158/1078-0432.CCR-1004-0022

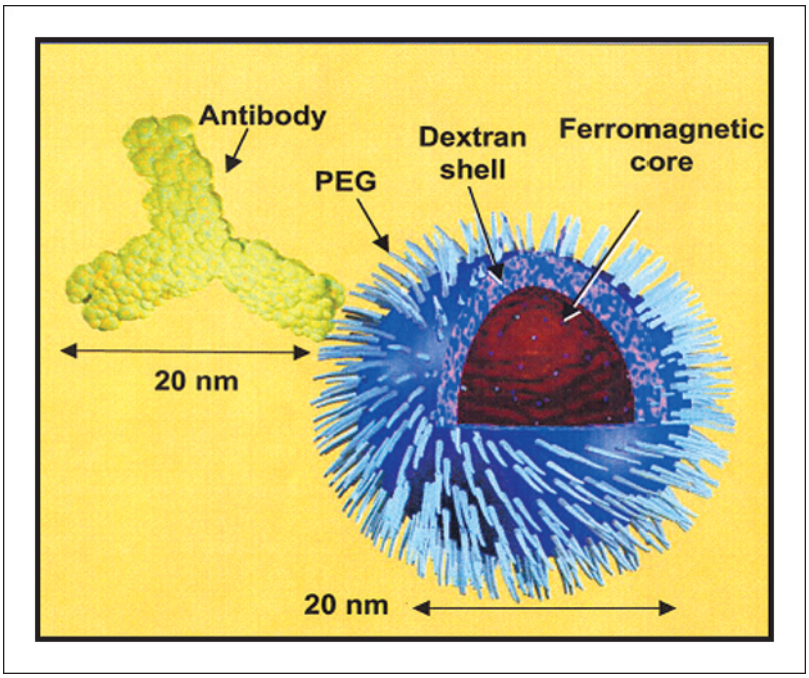

Fig. 1. Schematic of the bioprobes. ^{111}In-ChL6 bioprobes for AMF thermal ablation of cancer were prepared by ^{111}In-DOTA-ChL6 mAb conjugation to polyethylene glycol (*PEG*) on the dextran-coated iron oxide 20 nm nanoparticles (Nanomag-D spio beads) at one to two mAbs per nanoparticle.

describe development of the initial 20 nm ^{111}In-bioprobes, their pharmacokinetics in human tumor xenografted mice, tumor targeting at the cellular level by electron microscopy, and the efficacy and toxicity induced with various levels of external AMF in mice with human breast cancer xenografts.

Materials and Methods

Carrier-free ^{111}In (MDS Nordion, Ontario, Canada) was purchased as chloride in 0.05 mol/L HCl. Chimeric L6 (ChL6), human-mouse antibody chimera (Bristol-Myers Squibb Pharmaceutical Research Institute, Seattle, WA), reacts with an integral membrane glycoprotein highly expressed on human breast, colon, ovary, and lung carcinomas (5–8). ChL6 was specified as >95% pure monomeric immunoglobulin G by PAGE.

A high-gradient magnetic field column separator and nanomag-D-spio 20 nm nanoparticles with an iron oxide dextran matrix and polyethylene glycol COOH surface groups in 0.1 mol/L MES buffer (pH 6.3, 17 mg/mL) were obtained from micromod Partikeltechnologie GmbH (Rostock, Germany). MES, 1-ethyl-3-(3-dimethylaminopropyl)-carbodiimide HCl, *N*-hydroxysuccinimide, glycine, 2-iminothiolane (2IT), PBS (Sigma Chemical Co., St. Louis, MO), and 3,400 MW cutoff dialysis modules (Pierce, Rockford, IL) were purchased.

Radiolabeling and conjugation of ChL6 with 2-[p-(bromoacetamido)-benzyl]-DOTA. The immunoconjugate 2IT-BAD-ChL6 was prepared by conjugating 2-[*p*-(bromoacetamido)benzyl]-1,4,7,10-tetraazacyclododecane-*N*, *N*′,*N*″,*N*‴-tetraacetic acid (DOTA) (BAD) to ChL6 via 2IT as previously described (9). Final concentrations of 2.0 mmol/L, 15 mg/mL, and 1.3 mmol/L, respectively, were used in 0.1 mol/L tetramethylammonium phosphate (pH 9), at 37°C with 30-minute incubation. The 2IT-BAD-ChL6 conjugate was purified and transferred to 0.1 mol/L ammonium acetate (pH 5.3) by G50 molecular sieving chromatography. A mean of 1.3 DOTA groups were conjugated per ChL6 molecule. ^{111}In-chloride in 0.05 mol/L HCl (0.4 GBq) was buffered to a final pH of 5.3 in 0.1 mol/L ammonium acetate, and 2IT-BAD-ChL6 (4.0 mg) was added.

The solution was incubated for 30 minutes at 37°C, and then 0.1 mol/L sodium EDTA (Fisher Scientific, Pittsburgh, PA) was added to a final concentration of 10 mmol/L to scavenge nonspecifically bound ^{111}In. ^{111}In-2IT-BAD-ChL6 was purified from ^{111}In-EDTA by molecular sieving chromatography.

Purified ^{111}In-2IT-BAD-ChL6 was evaluated by cellulose acetate electrophoresis, molecular sieving high-performance liquid chromatography (SEC 3000), and RIA using HBT 3477 human breast cancer cells (10–13). ^{125}I-ChL6, lightly labeled and previously shown to be indistinguishable from ChL6, was assayed in parallel as a reference standard. High-performance liquid chromatography and cellulose acetate electrophoresis indicated that 100% and 97%, respectively, of ^{111}In-ChL6 were in monomeric form. The absolute binding in the live cell assays was 70% or more and 100% relative to the ^{125}I-ChL6 reference standard.

Conjugation of ^{111}In-DOTA-2IT-ChL6 with nanomag-D spio beads. Radiolabeled ^{111}In-DOTA-2IT-ChL6 was conjugated with 20 nm spio beads (nanoparticles) via amide linkage to the polyethylene glycol-COOH coating under conditions selected to retain the immunoreactivity of the final ^{111}In-ChL6 bioprobes. 1-Ethyl-3-(3-dimethylaminopropyl)-carbodiimide, 24.0 mg, and *N*-hydroxysuccinimide, 48 mg in 10 mL of 0.1 mol/L MES buffer, were mixed with 200 mg/12 mL of spio beads. This suspension was incubated for 1 hour at room temperature with continuous mixing, placed into 3,400 MW cutoff dialysis bags (each 12 mL), and dialyzed against 4 L of saline for 1 hour. ^{111}In-DOTA-2IT-ChL6 (1.3×10^{16} molecules; 4.6 mCi/3.2 mg/1.4 mL of saline) was transferred into 10 mL of 0.1 mol/L MES buffer, mixed with the activated spio bead suspension, and incubated for 1 hour at room temperature with continuous mixing (reaction ratio was 6.5×10^{13} molecules of mAb/mg of 20 nm spio beads). These conjugated ^{111}In-DOTA-2IT-ChL6-D-spio beads (20 nm), 32 mL, were again placed into four dialysis bags (3,400 MW cutoff; each 8.0 mL) and dialyzed against 4 L of saline at room temperature for 1 hour. The dialyzed product was mixed with 4.0 mL of 25 mmol/L glycine and mixed for 15 minutes to quench remaining active sites on the particle surface. The conjugated suspension was applied to the high-gradient magnetic field column separator using saline as both washing buffer and final eluent. The final suspension was collected from the magnetic column after removing it from the magnetic field. This suspension was brown with specific activity of 1.0 to 2.0 mCi/110 mg/20 mL (^{111}In-DOTA-2IT-ChL6-D-spio beads). Two microliters of final product were applied to multiple carcinoembryonic antigen strips for electrophoresis of 11 and 45 minutes and the immunoreactivity was evaluated in live

cell assay as described above. A bioprobe control lacking significant immunoreactivity (<20% of the ChL6 standard) was prepared in the same manner as above except that the glycine quench was omitted.

Mouse studies. Female (7-9 weeks old) athymic BALB/c *nu/nu* mice (Harlan Sprague-Dawley, Inc., Frederick, MD) were maintained according to University of California animal care guidelines on a normal diet *ad libitum* and under pathogen-free conditions. HBT 3477 cells were harvested in log phase; 3.0×10^6 cells were injected s.c. on the right side of the abdomen of each mouse. All studies were initiated 2 to 3 weeks after implantation when the mean tumor volume was 125 $\pm$ 44 mm^3. Studies were done using 20 to 30 μCi ^{111}In-ChL6 bioprobes injected i.v. into a lateral tail vein. ^{111}In-ChL6 bioprobe doses, 20 to 30 μCi (20 ng/2.2 mg ChL6/ bioprobe), were injected i.v. with 50 μg ChL6 in 200 μL saline. Concurrent with the therapy studies, 17 mice, 3 for each of 4 lots of immunoreactivity bioprobes used for therapy and 5 mice, given control nonimmunoreactive ^{111}In-ChL6 bioprobes, were sacrificed 48 hours after bioprobe injection and pharmacokinetic data obtained to determine if tumor uptake warranted therapy. In the pharmacokinetic studies, whole body activity was measured in a dose calibrator (CRC-12, Capintec, Inc., Pittsburgh, PA) immediately, and again after 1, 4, 24, and 48 hours, and values were expressed as percent injected dose. Blood activity, expressed as percent injected dose per milliliter, was determined by counting 2 μL blood samples, collected at 5 minutes, 1, 4, 24, and 48 hours after ^{111}In-ChL6 injection, in a γ well counter (Pharmacia LKB, Piscataway, NJ) calibrated using ^{111}In standards in the appropriate sample configuration and volumes. The mice were sacrificed 48 hours after the ^{111}In-ChL6 bioprobes and organs and tissue samples were collected. Activity, expressed as percent injected dose per gram, was measured in a γ well counter in a manner similar to that used for blood activity (14). Selected tumors were placed in Karnovsky's fixative for electron micrographic analysis of bioprobe location and tumor cell viability.

Bioprobe/AMF therapy was done in 32 mice, each bearing one tumor, randomized into three groups of 8 or 12 mice. In therapy studies, mice were treated with AMF 3 days after bioprobe injection. At that time, each mouse was anesthetized by injecting 0.02 mL i.p. per gram body weight of an anesthetic solution prepared by dissolving 0.5 g of 2,2,2-tribromoethanol in 1.0 mL of warm *tert*-amyl alcohol, then diluting the solution with 40 mL distilled water and filtering through a 0.2 μm filter.

After the mouse was anesthetized, four fiber optic temperature probes (FISO, Inc., Quebec, Canada) were placed to monitor tissue and core temperatures. One was inserted s.c. proximal to the lower spine by inserting a 16 gauge × 11/2 in. hypodermic needle at the base of the tail, and threading the fiber optic probe through the needle under the skin. This procedure was repeated for a second probe placed s.c. near the tumor. A third probe was taped onto the skin of a hind limb using wound dressing, and a fourth probe was inserted 1 cm into the rectum. After the probes were in place, the mouse was wrapped lightly in absorbent paper and inserted into a 50 mL centrifuge tube from which the bottom had been removed. The tube and mouse were inserted into the felt-lined AMF coil so that the tumor was positioned in a 1-cm-high amplitude region of the induction coil. Once the mouse was in place and the parameters programmed into the controls, the AMF generator was turned on. AMF was applied in the coil with amplitudes of 1,300 Oe (n = 12), 1,000 Oe (n = 8), or 700 Oe (n = 12), as described below. AMF parameters (i.e., amplitude, duration, and nature of exposure) were selected to minimize nonspecific tissue heating due to the production of eddy currents, yet provide sufficient energy to activate the bioprobes in the region of the tumor to create localized heating. The AMF system was designed to produce an inhomogeneous high amplitude AMF in a 1-cm-wide band in the tumor region. Reported AMF amplitudes were measured in this 1-cm region and represent AMF amplitudes at only the tumor location. AMF amplitudes were substantially lower for all instrument settings outside this region and are not reported. Data used for the choice of parameters were obtained in an earlier study (15), which also contains a detailed description of AMF equipment and methods. After exposure, each mouse was left in the coil until the core (rectal) temperature began to decrease, then all probes were removed. The mouse was removed from the coil and centrifuge tube and placed on a warm recovery pad. When the righting reflex returned, the mouse was returned to its cage.

The results from a previously conducted study to determine the parameters for safe application of high amplitude AMF (15) were used to select AMF levels for the bioprobe treatment herein. Response was evaluated for groups of mice receiving no treatment and cohorts treated at each of three magnetic field (energy) levels. These three groups of mice were followed for tumor growth and body weight thrice per week for 12 weeks. Tumors were measured with calipers in three orthogonal directions and the volume was calculated using the formula for a hemiellipsoid (16). Tumor effects were analyzed by Wilcoxon rank-sum comparison of time to double, triple, and quintuple tumor volume in each AMF treatment group. Twenty-five additional control mice in three groups were followed in the same manner described above: one group of five mice received AMF but no bioprobes; one group of five mice received ^{111}In-ChL6 bioprobes but no AMF; and a third group of 15 mice received no treatment.

Tumors were harvested from three mice in the pharmacokinetics group and three mice treated with bioprobes and 1,000 or 1,300 Oe. These were placed in Karnovsky's fixative for ultrastructural analysis of bioprobe location and cancer cell viability. They were then fixed in osmium tetroxide and embedded in an Epon-like resin using standard protocols (17). Ultrathin sections were viewed on a Philips CM120 Biotwin.

Results

The final ^{111}In-ChL6-bioprobe products were brownish suspensions without precipitate. Four bioprobe preparations and one control preparation are represented in the reported work. The concentration of the beads was estimated by UV/visible spectrophotometry at a wavelength of 492 nm using unconjugated beads as a reference, and protein concentration was estimated at a wavelength of 280 nm. Specific activity of the ^{111}In-DOTA-2IT-ChL6 bioprobes was 7 to 20 μCi/ChL6 (4.4×10^{13} molecules)/164 μL/mg of nanoparticles. The cellulose acetate electrophoresis of the preparations at 11 and 45 minutes revealed 94% to 98% and 91% to 97% monomeric final product at 11 and 45 minutes, respectively. ^{111}In-ChL6 bioprobe products bound *in vitro* to HBT 3477, 50% to 70% relative to the ^{111}In-ChL6 standard (13), except that the bioprobe control, produced without glycine quenching, bound only 20% relative to the standard.

Pharmacokinetics. Blood clearances for the ^{111}In-ChL6 bioprobes are shown in Fig. 2A. Liver and spleen uptakes (percent injected dose per gram) at 48 hours were twice the uptakes previously observed for ^{111}In-ChL6 (14). Tumor, lung, kidney, and marrow uptakes of the ^{111}In-ChL6 bioprobes, however, were not different than that previously reported for ^{111}In-ChL6. Tumors from mice receiving the nonimmunoreactive bioprobe control showed no bioprobe uptake 48 hours postinjection, faster blood clearance, and similar normal organ uptake (Fig. 2).

Toxicity. After slight weight loss associated with the procedure, the average weights of treated and untreated mice were equivalent throughout the 84-day trial. Death occurred acutely (within 24 hours) in 4 of 12 mice which had been treated at 1,300 Oe. Acute erythematic skin changes were also noted in mice treated at this level. Toxicity was not observed in the other groups.

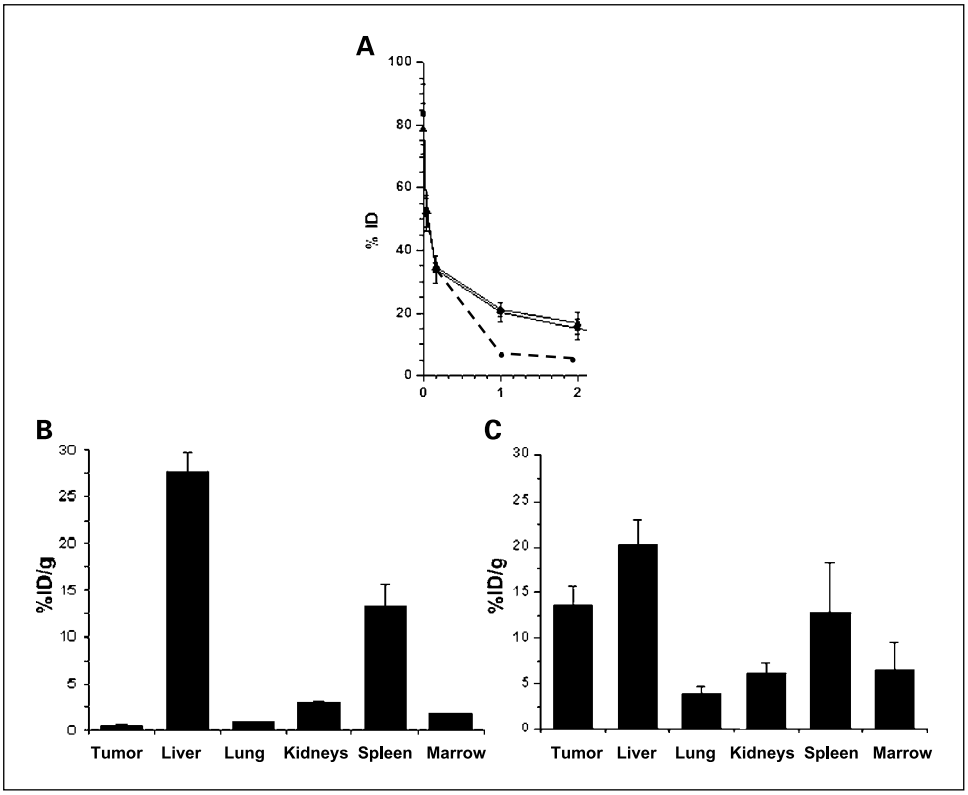

Fig. 2. Pharmacokinetic studies of ^{111}In-ChL6 bioprobes and a ^{111}In-ChL6 bioprobe control (nonimmunoreactive). *A*, blood clearance of ^{111}In-ChL6 bioprobes (*solid lines*) showed 20% and 18% ID in the blood at 24 and 48 hours, respectively, for mice in the pharmacokinetics group and mice in the AMF therapy group. The nonimmunoreactive bioprobe control group (*dashed line*) showed more rapid blood clearance. *B*, pharmacokinetics of the nonimmunoreactive ^{111}In-ChL6 bioprobe control in mice with HBT 3477 tumors, sacrificed at 48 hours postinjection. When compared with the immunoreactive ^{111}In-ChL6 bioprobes (*C*), organ uptake was similar but there was no tumor targeting of the control bioprobes. *C*, pharmacokinetics of immunoreactive ^{111}In-ChL6 bioprobes in HBT 3477 – bearing mice sacrificed at 48 hours postinjection. Concentrations in the liver (20 ± 2.1) and spleen (12.9 ± 5.3) were twice those previously seen with ^{111}In-ChL6 alone (14). However, tumor (13.7 ± 2.1% ID/g), lung (3.9 ± 0.8% ID/g), kidney (6.2 ± 1.3% ID/g), and marrow (6.6 ±3.0% ID/g) uptakes of ^{111}In-ChL6 bioprobes were similar to that previously reported for ^{111}In-ChL6.

Efficacy. Initial tumor volume was defined as the volume on the day before treatment. Mean tumor volume for any given day after treatment was calculated from actual measurements on that day or from values derived from linear interpolation if that day fell between actual measurements. Normal tumor growth was evaluated for mice receiving no treatment. Tumor effect was analyzed by Wilcoxon rank-sum comparison of the doubling, tripling, and quintupling time for individual tumors in each test group compared with individual tumors in the untreated control group. Tumors in all of the groups receiving bioprobes and AMF had a statistically decreased tumor growth rate with significantly higher mean time to triple or quintuple tumor volume than those in untreated control tumors (Table 1; Fig. 3). Mean time to doubling showed response as well but statistically was not as robust. Many tumors showed regression but no tumors had complete regression.

Electron micrographs. Electron micrographic evaluation of tumors taken at 48 hours after injection of the ^{111}In-ChL6 bioprobes showed easily detectable bioprobes on tumor cell membrane surfaces (Fig. 4A). Noteworthy also is the healthy appearance of the cancer cells. Tumors harvested 5 days after bioprobe injection and 48 hours after AMF treatment showed tumor cell necrosis (Fig. 4B). Thus, the bioprobes not only reached the tumor but also bound to targets on the tumor cell surface. Response to AMF was associated with widespread tumor cell necrosis on electron microscopy.

Discussion

This study confirms immunotargeting of bioprobes to human breast cancer tumors *in vivo* using ^{111}In-mAb linked to the nanoparticles to produce bioprobes. The radioactive tracer provided a means to ensure that adequate tumor delivery had occurred before giving AMF to achieve thermal ablative therapy. Thus, thermomagnetic bioprobes, systemically delivered to metastatic tumor with delivery monitored by radioimmunoimaging, may provide a safe and effective approach to develop AMF thermal ablation.

Table 1. Decreased tumor growth rate related to Oersted treatment level

Oe	*n*	Mean	SD	Two-sided *P*
(*A*)				
1,300	12	35	28	0.0277
1,000	8	32	19	0.0300
700	12	29	23	0.1194
All treated	12	35	28	0.0114
Control	14	13	7	
(*B*)				
1,300	12	49	27	0.0335
1,000	8	50	25	0.0206
700	12	45	19	0.0029
All treated	32	48	24	0.0013
Control	14	24	9	

NOTE: Mean time for the HBT 3477 human breast xenografts to triple (*A*) and quintuple (*B*) in volume segregated by oersted treatment group. Two-sided *P* values when compared with control group (Wilcoxon-Mann-Whitney test). The decrease in tumor growth rate was related to the oersted level received by that cohort and was significant ($P \leq 0.05$) for most groups.

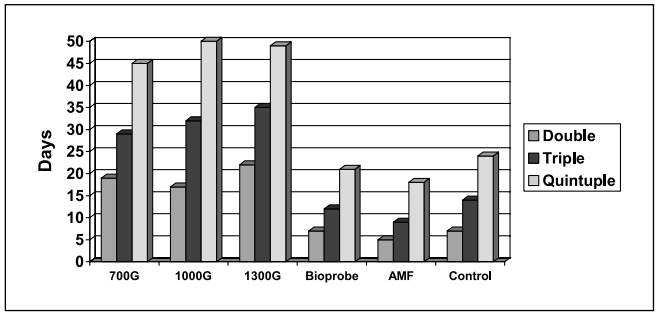

Fig. 3. Efficacy is reflected by tumor regression in all of the treated groups (decrease in growth rate). A statistically significant decrease in mean tumor growth rate ($P = 0.0013$ for all treated tumors compared with untreated tumors), with higher mean time to triple and quintuple tumor volume than for the untreated tumors, was observed. Tumor effect was analyzed by Wilcoxon rank-sum comparison of the doubling, tripling, and quintupling time for individual tumors in each test group compared with individual tumors in the untreated control group (see Table 1).

Prior pharmacokinetic studies with ^{111}In-ChL6 in athymic mice bearing HBT 3477 xenografts showed excellent tumor targeting (14) that was successfully translated into breast and prostate cancer imaging and therapy protocols for patients (18, 19). Therefore, this model was considered an appropriate tool for initial *in vivo* bioprobe studies. Because the nanoparticles were assembled with dextran coating on the iron oxide magnetic core and a brush border of stabilizing polyethylene glycol polymer on the surface, covalent conjugation of one to two mAbs per nanoparticle could be achieved using carbodiimide activation of the carboxyl ends of the polyethylene glycol brush border (Fig. 1). This chemistry provided both immunoreactive mAb and a stable link to the nanoparticle. ^{111}In-DOTA conjugated to the mAb before bioprobe linkage facilitated assurance of tumor binding of the ^{111}In-bioprobes *in vivo*. Furthermore, by providing *in vivo* pharmacokinetics before AMF and thereby assuring tumor uptake, the effects of variations in AMF could be evaluated and the time for application of AMF could be selected. Obviously, quantitative imaging in patients could be used in future applications to derive this information.

Compared with previously published nanoparticle studies (20, 21), the ^{111}In-ChL6 bioprobes remained substantially longer in the circulation and had substantially higher tumor uptake. The time that the ^{111}In-ChL6 bioprobes remained in circulation provided ample opportunity for these 20 nm particles to exit the blood and access the cancer cells. Evidence of the delivery of these bioprobes to the membranes of the cancer cells was provided by electron micrographs of tumors removed 48 hours after injection (Fig. 4A). Electron micrographs also provided indirect evidence for the stability of the bioprobes as an intact immunotargeting unit in mice. The tumor uptake of

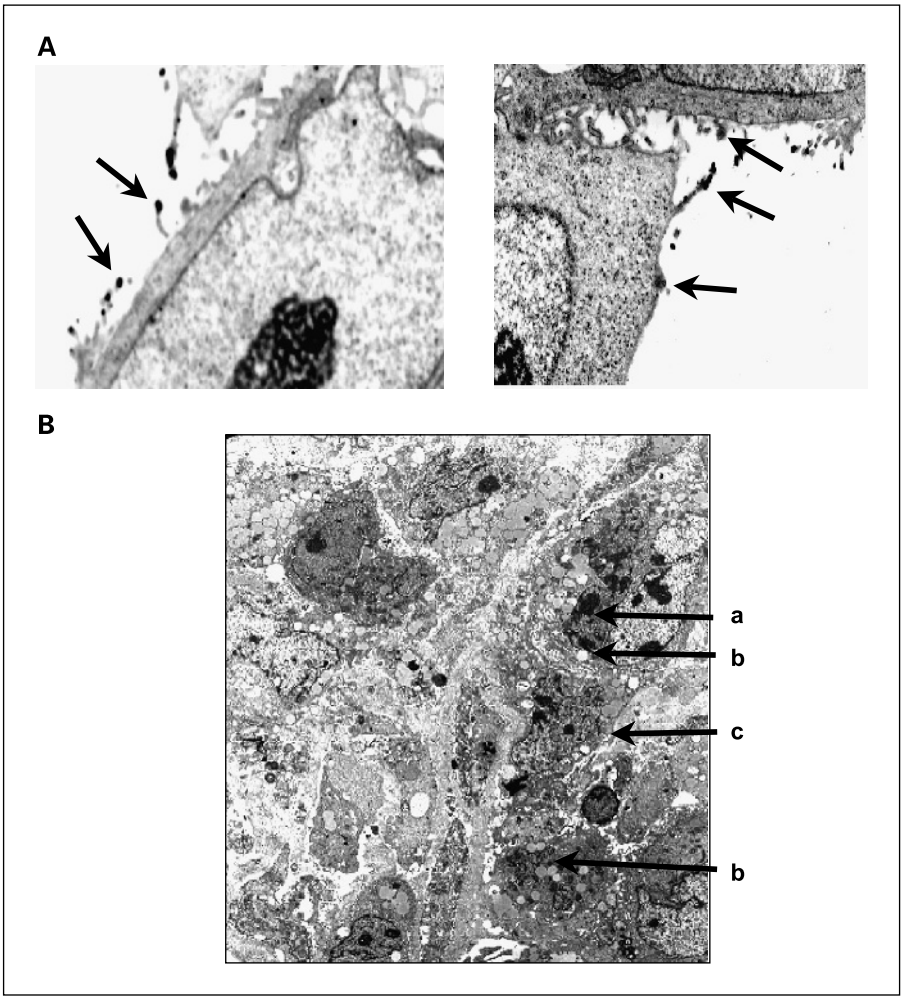

Fig. 4. The electron micrographs [original magnification factor: 2.7 (6,500) = 17,550] of HBT 3477 xenograft tumors which had been excised from the mice, at the time of sacrifice for biodistribution study, 48 hours postinjection (*A*): Intact bioprobes can be seen on the cancer cell surfaces (*arrows*) inferring cell binding and retention; nuclear membrane and nucleolus are clearly seen in these untreated cells. *B*, electron micrographs 120 hours after bioprobe injection, 48 hours after AMF treatment at 1,300 Oe, demonstrating substantial necrosis of the cancer cells (*a*, nuclei of cells seen as fragments; *b*, abundant cytoplasmic vacuoles; *c*, disintegration of cell and nuclear membranes).

^{111}In-ChL6 bioprobes, when compared with prior studies of ^{111}In-ChL6 in this mouse model, was gratifyingly similar. This study also showed that mAb targeted nanoparticles can be produced, purified, characterized, and targeted to cancer cells *in vivo* in sufficient amounts to cause cancer cell necrosis from thermal ablation after externally applied AMF. New bioprobes with nanoparticles having enhanced thermal magnetic properties are under development. Iron toxicity is a consideration in the development of bioprobe therapy, but is unlikely. Clinical experience with parenteral iron preparations suggests that iron doses and forms, considered integral to this thermal ablative therapy, should be well tolerated.

In conclusion, the study presented here showed tumor regression at all AMF levels applied after bioprobes were delivered to the cancer cells. Tumors did not respond to AMF or bioprobes alone, and immunoreactive bioprobes were necessary to get *in vivo* targeting of the cancer cells. In groups where applications of 700 or 1,000 Oe were given, no toxicity was observed. These initial studies show the promise for this new cancer therapy modality.

References

1. Overgaard J. History and heritage—an introduction. In: Overgaard J, editor. Hyperthermia Oncology. London: 2 Taylor and Francis; 1985.
2. Streffer C. The biological basis for tumor therapy by hyperthermia and radiation. In: Streffer J, editor. Hyperthermia and the therapy of malignant tumors. Berlin: Springer; 1987.
3. Hildebrandt B, Wust P, Ahlers O, et al The cellular and molecular basis for hyperthermia. Crit Rev Oncol Hematol 2002;43:33–56.
4. Moroz P, Jones SK, Gray BN. Magnetically mediated hyperthermia: Current status and future directions. Int J Hyperthermia 2003;18:267–84.
5. Fell HP, Gayle MA, Yelton D, et al. Chimeric L6 antitumor antibody. Genomic construction, expression, and characterization of the antigen binding site. J Biol Chem 1992;267:15552–8.
6. Liu AY, Robinson RR, Hellstrom KE, Murray EDJ, Chang CP, Hellstrom I. Chimeric mouse-human IgG1 antibody that can mediate lysis of cancer cells. Proc Natl Acad Sci U S A 1987;84:3439–43.
7. Hellstrom I, Horn D, Linsley P, Brown JP, Brankovan V, Hellstrom KE. Monoclonal antibodies raised against human lung carcinomas. Cancer Res 1986;46:3917–23.
8. Marken JS, Bajorath J, Edwards CP, et al. Membrane topology of the L6 antigen and identification of the protein epitope recognized by the L6 monoclonal antibody. J Biol Chem 1994;269:7397–401.
9. McCall MJ, Diril H, Meares CF. Simplified method for conjugating macrocyclic bifunctional chelating agents to antibodies via 2-iminothiolane. Bioconjug Chem 1990;1:222–6.
10. DeNardo SJ, DeNardo GL, Kukis DL, et al. ^{67}Cu-2IT-BAT-Lym-1 pharmacokinetics, radiation dosimetry, toxicity and tumor regression in patients with lymphoma. J Nucl Med 1999;40:302–10.
11. Moi MK, Meares CF, DeNardo SJ. The peptide way to macrocyclic bifunctional chelating agents: synthesis of 2-(*p*-nitrobenzyl)-1,4,7,10-tetraazacyclododecane-*N*,*N*′,*N*″,*N*‴-tetraacetic acid and study of its yttrium (III) complex. J Am Chem Soc 1988;110:6266–7.
12. Kukis DL, DeNardo SJ, Mills SL, Shen S, O'Donnell RT, DeNardo GL. Stability of monoclonal antibodies, Lym-1 and ChL6, and 2IT-BAD-Lym-1 immunoconjugate with ultra freezer storage. Cancer Biother Radiopharm 1999;14:363–9.
13. Kukis DL, DeNardo GL, DeNardo SJ, et al. Effect of the extent of chelate substitution on the immunoreactivity and biodistribution of 2IT-BAT-Lym-1 immunoconjugates. Cancer Res 1995;55:878–84.
14. DeNardo SJ, Burke PA, Leigh BR, et al. Neovascular targeting with cyclic RGD peptide (cRGDf-ACHA) to enhance delivery of radioimmunotherapy. Cancer Biother Radiopharm 2000;15:71–9.
15. Ivkov R, DeNardo SJ, Daum W, et al. Application of high amplitude alternating magnetic fields for heat induction of nanoparticles localized in cancer. Clinical Cancer Research 2005;11:7093s–103s.
16. DeNardo SJ, Kukis DL, Miers LA, et al. Yttrium-90-DOTA-peptide-chimeric L6 radioimmunoconjugate: efficacy and toxicity in mice bearing p53 mutant human breast cancer xenografts. J Nucl Med 1998;39:842–9.
17. Hayat MA. Principles and techniques of electron microscopy: biological applications. 3rd ed. Boca Raton: CRC Press; 1998.
18. DeNardo SJ. Radioimmunotherapy for breast cancer: Systemic tumor-targeted irradiation. Advances in Oncology 1999;15:23–9.
19. DeNardo SJ, Richman CM, Goldstein DS, et al. Yttrium-90/Indium-111-DOTA-peptide-Chimeric L6: pharmacokinetics, dosimetry and initial results in patients with incurable breast cancer. Anticancer Res 1997;17:1735–44.
20. Jordan A, Scholz R, Wust P, Fahling H, Felix R. Magnetic fluid hyperthermia (MFH): cancer treatment with AC magnetic field induced excitation of biocompatible superparamagnetic nanoparticles. Journal of Magnetism and Magnetic Materials 1999;201:413–9.
21. Jordan A, Wust P, Scholz R, et al. Cellular uptake of magnetic fluid particles and their effects on human adenocarcinoma cells exposed to AC magnetic fields *in vitro*. Int J Hyperthermia 1996;12:705–22.